Electronic structure of the Mo(001) surface

S. C. Hong
Physics Department, University of Ulsan, Ulsan 680-749, Korea

J. W. Chung
Physics Department and the Basic Science Research Center, Pohang Institute of Science and Technology, Pohang 790-330, Korea

(Received 9 December 1992; revised manuscript received 22 February 1993)

We report computed results of the surface band structures of a molybdenum (001) surface by employing a self-consistent semirelativistic version of the full potential linearized augmented-plane-wave method. Computation was carried out for a seven-layer slab of bulk-truncated (1×1) Mo(001) surface, ignoring the spin-orbit interaction. The resulting surface band structures are compared with recent experimental measurements at temperatures above and below a transition temperature. Despite general agreement with observation, we noted some characteristic differences in both energy and band connectivity. Details in both the electronic properties of surface states and resonances are examined and discussed in light of their significance for reconstruction mechanism.

I. INTRODUCTION

Understanding the nature of the anomalously intense surface state (SS), known as the Swanson hump (SH) state, located just below the Fermi energy (E_F), observed on Mo(001) and W(001) surfaces,[1] has been a subject of theoretical interest for several years.[2–10] The origin of the large density of states of the SH is quite interesting in its own right. Beside the instabilities of these surfaces, which induce reconstructions upon cooling,[11,12] a possible role of the SH in driving reconstructions could be an additional stimulating research topic.[2–10,13–18]

The subtle nature of the problem resides in the fact that the two surfaces exhibit distinctly different reconstructed structures below the transition temperatures (T_c) despite the similarity of their lattice structures and isoelectronic properties above T_c. The reconstructed structures of W(001) and Mo(001) have been characterized as a commensurate $c(2\times2)$ and an incommensurate $c(2.2\times2.2)$ phase, respectively. Previous studies of these surfaces have concentrated into two categories: One is to characterize changes in the lattice structures accompanying the transitions, while the other is to clarify a driving mechanism for the transitions. For W(001), such important properties of the transition are believed to be relatively well documented compared to Mo(001).

In our earlier paper,[16] we reported that reconstruction of the Mo(001) surface is driven essentially by a Peierls-type instability with a wave vector of reconstruction $q=2\mathbf{k}_{\parallel}^{F}=1.30$ Å^{-2}, in close agreement with previous low-energy electron-diffraction (LEED) observations[11,12,19] and recent studies of a Kohn anomaly along the symmetry line $\bar{\Sigma}$ or (11) direction of the surface Brillouin zone (SBZ).[20,21] This conclusion was based on the fact that the two-dimensional Fermi-surface contour changes its curvature upon cooling below T_c, indicating a good possibility of Fermi-surface nesting at T_c. This nesting, which occurs in the direction perpendicular to the $\bar{\Sigma}$ line extending about 0.3 Å^{-1}, can greatly enhance electronic susceptibility and may be enough to induce the transition with strong coupling between nonadiabatic electrons near E_F and a suitable phonon mode.

We also reported experimentally determined energy dispersion relations of SS's and surface resonances (SR's) in the $\bar{\Sigma}$ and $\bar{\Delta}$ directions at temperatures above and below T_c.[18] These experimental surface band structures and the symmetries of the states show several important differences with previous studies[2,3,9] in the energies, band connectivity, and Fermi wave-vector ($\mathbf{k}_{\parallel}^{F}$) dimensions throughout the SBZ.

Motivated by these experimental observations,[14–16,18] which reveal deviations from previous calculations, we carried out a calculation of surface band structures employing the full-potential linearized augmented-plane-wave method (FLAPW) that includes all relativistic corrections except spin-orbit interaction. We thus present a self-consistent band structure for a Mo(001) surface by FLAPW, and compare it with recent experiments. We also present wave-function symmetries of surface states as well as distributions of the local density of states in each layer of the slab. The results qualitatively agree with experimental findings except for several features that might originate from the reconstruction itself. However, unlike the previous calculations,[2,3,9] no relaxation is required to produce such surface states, but self-consistency is found to be essential in obtaining a precise work function of 4.24 ± 0.20 eV, in excellent agreement with the experimental value of 4.4 ± 0.20 eV.[18]

II. METHOD OF CALCULATION

To investigate the electronic structure of the Mo(001) surface, the surface is approximated by a single slab consisting of seven unreconstructed and unrelaxed layers of Mo(001). The Kohn-Sham equations are solved self-consistently in the local-density approximation (LDA) by

employing the FLAPW method, where no shape approximations are made for the potential or the charge density in solving Poisson's equation. All the matrix elements corresponding to this general potential were rigorously taken into account in all parts of space. Lattice harmonics with angular momentum up to $l=8$ were used to expand the charge density and potential, and also to construct the wave functions inside a muffin-tin sphere.

The explicit form of Hedin and Lundqvist was used for the exchange-correlation potential. The core electrons were treated fully relativistically, whereas the valence electrons were treated semirelativistically, i.e., including all relativistic terms except the spin-orbit interaction. About 2×320 basis functions were used for each of the 36 k points in the $\frac{1}{8}$ irreducible wedge of the SBZ. Self-consistency was assumed when the rms difference between the input and output charge densities was less than 3×10^{-4} electrons/(a.u.)^3.

III. RESULTS AND DISCUSSION

A. Surface charge density and work function

The charge density is the basic physical quantity in LDA theory, which provides insight into the formation of a surface. Figure 1 shows valence charge-density contours in a (110) plane for positive z, where Mo(S), Mo($S-1$), and Mo(C) represent the surface, subsurface, and center molybdenum layers, respectively. The contour lines are drawn in logarithmic scale with adjacent lines differing by a factor of $\sqrt{2}$. It is seen that the valence charge density decreases smoothly as one moves away from the surface into the vacuum, while it rapidly changes into a bulklike shape inside the film, indicating a short metallic screening length. This overall feature is quite similar to that of the W(001) surface.[7,8]

In order to describe the charge configurations quantitatively, we present the number of conduction electrons within the muffin-tin spheres in Table I, as decomposed into different angular-momentum contributions. As given in Table I, the similarity of the charge configurations of a subsurface atom and a center-layered atom suggests a screening length on the order of the atomic spacing. One can also figure out the essential features of bonding characteristics in Fig. 1. i.e., the fairly well-localized lobes of the xy-, yz-, and xz-type d orbitals for the interior atoms weaken significantly toward the missing nearest neighbors for the surface atoms. The delocalized s and p electrons spill out into the vacuum to reduce their kinetic energy and smooth out the discontinuity at the surface. The spill-out charge density forms a dipole layer, which sensitively determines the work function, here 4.24 eV.

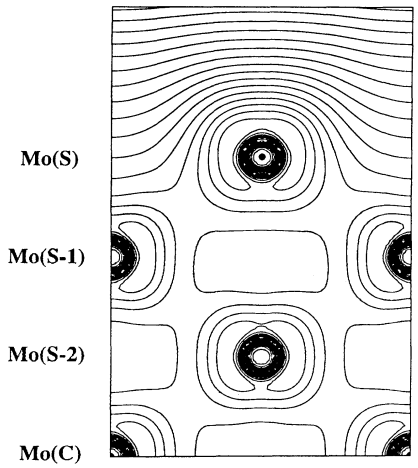

FIG. 1. Distribution of valence charge-density contours in the (110) plane. The contour lines are drawn in logarithmic scale with adjacent lines differing by a factor of $\sqrt{2}$.

TABLE I. Number of valence electrons inside the muffin-tin spheres, as decomposed into different angular-momentum components. Here, Mo(S), Mo($S-1$), and Mo(C) denote the surface, subsurface, and center molybdenum layers, respectively. Note the close similarity of charge configurations between Mo($S-1$) and Mo(C), indicating a short metallic screening length of about the atomic spacing.

	s	p	d	Total
Mo(S)	0.308	0.179	3.682	4.208
Mo($S-1$)	0.362	0.365	3.729	4.537
Mo($S-2$)	0.360	0.382	3.726	4.544
Mo(C)	0.359	0.383	3.736	4.544

B. Single-particle spectra and surface states

The calculated band structure along the high-symmetry lines of the irreducible part of the SBZ is presented in Fig. 2 for the states of even (a), and odd (b) mirror reflection symmetries with respect to the given symmetry lines. Dotted (dashed) lines correspond to even (odd) parity with respect to the z reflection. The solid circles indicate SS or SR, which are identified from their charge localization in the surface layer. A true SS has most of its charge residing in the surface layer and decays rapidly into the bulk, while a SR has a significant portion of its charge in the surface layer, but still penetrates into the bulk and mixes with bulk bands. Although the overall feature of the band structure agrees qualitatively with previous experiments[14–16,18] and theoretical calculations,[2,3,9] we notice several distinctly different characteristics for the occupied states, as discussed below.

The most important difference is found for the SS just below E_F along the $\bar{\Sigma}$ symmetry line. This state is a main source of the strong SH in the angle-resolved photoemission spectrum at the zone center ($\bar{\Gamma}$) of the SBZ. We find three $\bar{\Sigma}_1$ SS's at $\bar{\Gamma}$, only one of which is occupied, in contrast to W(001), where all three are occupied.[7,8,10] Experimentally, the occupied $\bar{\Sigma}_1$ SS is found to form a flat band with a fairly small dispersion of less than 0.3 eV, and stays strong before it crosses E_F at $\mathbf{k}_\parallel^F=0.65$ and 0.59 Å^{-1} along the $\bar{\Sigma}$ and $\bar{\Delta}$ lines, respectively.[16,18] The state actually crosses E_F at different Fermi wave vectors throughout the irreducible SBZ so that one may construct a closed two-dimensional (2D) Fermi-surface contour.[16]

Our calculation shows two flat $\bar{\Sigma}_1$ SS bands with the band of even parity with respect to z reflection occupied, and that of odd parity unoccupied. This flat feature is in good accord with recent experiments,[16,18] and has never been produced in previous calculations[2,3,9] regarding energies, and band extension. Our calculation, however, fails to predict exact E_F crossings, or to produce the rather long extension of the flat band along the $\bar{\Delta}$ line observed for a reconstructed Mo(001) surface.[16,18] In contrast, a self-consistent pseudopotential calculation by Kerker, Ho, and Cohen[3] predicts a flat band extending about one-third of the way to the zone boundary $\bar{X}$ along $\bar{\Delta}$, but fails to produce the corresponding band along $\bar{\Sigma}$.

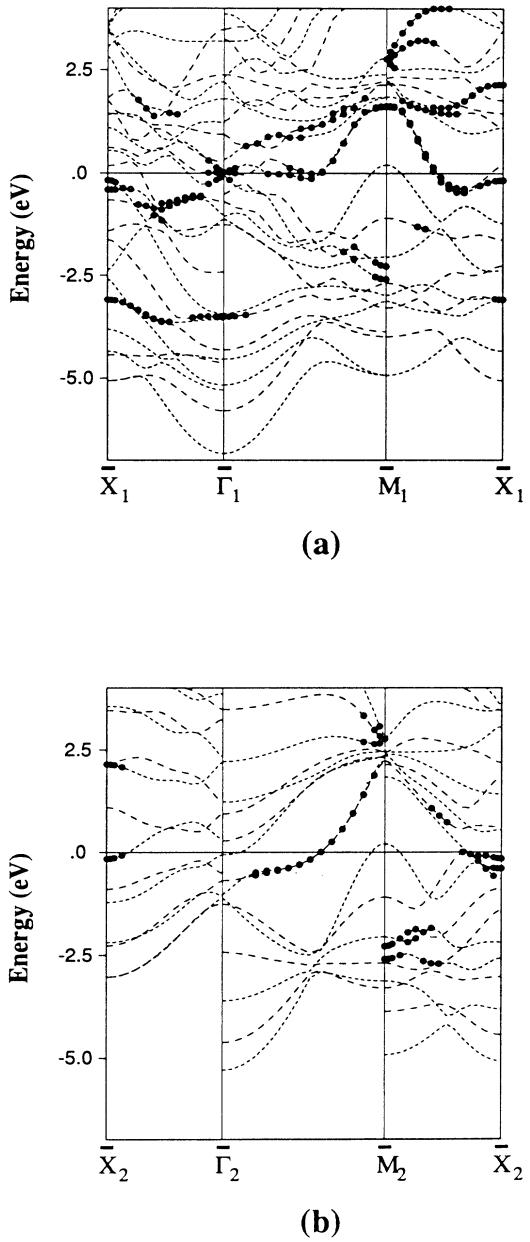

FIG. 2. Calculated surface dispersion relations for the states of even (a), and odd (b) mirror reflection symmetries with respect to the given symmetry lines ($\bar{\Sigma}$, $\bar{\Delta}$, and $\bar{Y}$). The solid circles indicate SS or SR for which more than half of their charges are localized in the surface layer. Dotted (dashed) lines correspond to even (odd) parity with respect to the z reflection.

Contour plots of the charge density for the $\bar{\Sigma}_1$ SS in a (110) plane are presented in Fig. 3 at $\mathbf{k}_\parallel = 0$ Å^{-1} with binding energy $E_b = +0.02$ eV [(a); unoccupied] and $\mathbf{k}_\parallel = 0.65$ Å^{-1} with $E_b = -0.12$ eV [(b); occupied], revealing the $d_{3z^2-r^2}$, and d_{xy}, d_{xz+yz} orbital characters, respectively. Although not shown in the figure, a contour plot of charge density in a (001) surface plane at $\mathbf{k}_\parallel = 0.65$ Å^{-1} also shows a clear d_{xy} orbital character. As seen in Fig. 3, the $\bar{\Sigma}_1$ SS is well localized in the surface layer, and is expected to be altered significantly through reconstruction. This is, in fact, observed experimentally as evidenced by enhanced spectral intensity at temperature below T_c (see Fig. 4 in Ref. 16).

As in previous calculations, we find two closely spaced $\bar{\Sigma}_2$ SR states (even and odd parity each) near E_F with upward dispersion along $\bar{\Sigma}$. The two SR states overlap each other before crossing E_F at $\mathbf{k}_\parallel = 0.84$ Å^{-1}, and become unoccupied states showing a rather large dispersion of about 2.0 eV. The E_F crossing differs with the experimental value of $\mathbf{k}_\parallel = 0.65$ Å^{-1},[16] but agrees well with the previous calculation of Stephenson and Bullett.[9]

These $\bar{\Sigma}_2$ SR states are found to be fairly well localized on the outermost layer, and thus are expected to have a significant role in driving the reconstruction, as suggested previously.[16,18,21] Theoretically, it has been suggested that these $\bar{\Sigma}_2$ SR states can lower the total electronic energy by splitting into bonding-antibonding states at the new zone boundary through the reconstruction.[9,21] However, no clear experimental evidence for such a splitting has been reported. A contour plot of the charge density for the $\bar{\Sigma}_2$ SR of -0.30 eV at $\bar{k}_\parallel = 0.65$ Å^{-1} in a (110) mirror plane exhibits the predominant $d_{x^2-y^2}$, and d_{xz-yz} orbital characters, as shown in Fig. 4.

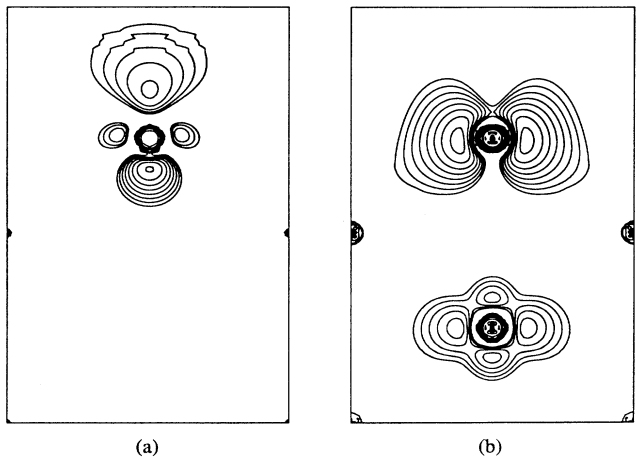

FIG. 3. Contour plots of charge density for the $\bar{\Sigma}_1$ SS in a (110) plane at $\mathbf{k}_\parallel = 0$ Å^{-1} with binding energy $E_b = +0.02$ eV (a) and $\mathbf{k}_\parallel = 0.65$ Å^{-1} with $E_b = -0.12$ eV (b) states. The unoccupied (a) and occupied (b) states show the $d_{3z^2-r^2}$, and d_{xy}, d_{xz+yz} orbital characters, respectively.

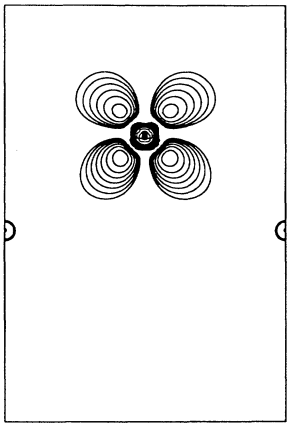

FIG. 4. Charge density of the $\bar{\Sigma}_2$ SR at $\mathbf{k}_{\parallel}=0.65$ Å^{-1} with $E_b=-0.30$ eV in a (110) plane perpendicular to surface. Subsequent contour lines differ by a factor of $\sqrt{2}$.

Another interesting feature along $\bar{\Sigma}$ is that there exist two low-lying $\bar{\Sigma}_1$ SR near $\bar{M}$, with downward dispersions for increasing $\mathbf{k}_{\parallel}$, and a low-lying $\bar{\Sigma}_1$ SR near $\bar{\Gamma}$ with almost flat dispersion, in excellent agreement with experiments.[16,18] The charge contours for the low-lying $\bar{\Sigma}_1$ SR at $\bar{M}$ (not shown) are found to reveal a d_{xy} orbital character that is strongly hybridized with the next nearest neighbors. The lower $\bar{\Sigma}_1$ SR of even parity is much more localized on the surface than the upper odd-parity state.

Now, looking into the dispersions along the $\bar{\Delta}$ line, we find other minor conflicts between our results and experiment[16,18] for the $\bar{\Delta}_1$ SS and the $\bar{\Delta}_1$ SR near E_F. Experimentally, two nearly flat bands, a $\bar{\Delta}_1$ SS of $E_b=-0.2$ eV and a $\bar{\Delta}_1$ SR of $E_b=-0.6$ eV, were observed for the reconstructed surface.[18] These states disperse within 0.2 eV and extend more than halfway along $\bar{\Delta}$, running almost parallel with each other. Similar dispersions were also observed for the surface above T_c.[14,15,18]

Our results in Fig. 2 are slightly different from these observations with regard to energies and band extensions. However we find that the origin of the experimentally observed $\bar{\Delta}_1$ SS which crosses E_F at $\mathbf{k}_{\parallel}=0.3$ Å^{-1} along $\bar{\Delta}$ is the occupied SS of $E_b=-0.12$ eV at $\bar{\Gamma}$. The degree of extension of the $\bar{\Delta}_1$ SS in numerous previous calculations has been controversial with predictions of the E_F crossing in the range of 0.3–0.5 Å^{-1}.[2,3,9] Interestingly, unlike the previous calculations,[2,3] our results correctly predict the existence of a SS band of mixed symmetry near $\bar{X}$, in good accord with recent experiments.[14,16,18]

We note that the $\bar{\Delta}_1$ SR which disperses downward about 0.4 eV in Fig. 2 actually consists of two closely spaced bands, with even and odd parity. Similar to the $\bar{\Sigma}_2$ SR, these $\bar{\Delta}_1$ SR should also be affected by reconstruction, because of their charge localization on the outermost layer. Another $\bar{\Delta}_1$ SR of -3.2 eV at $\bar{X}$ with downward dispersion of about 0.6 eV is found, which extends almost all the way to $\bar{\Gamma}$, as observed experimentally.[14,16,18]

One finds several occupied SS bands along the $\bar{Y}$ symmetry line, which are believed to exist in the absolute symmetry gaps in this region (see Refs. 2 and 3). The high-lying SS near $\bar{X}$ of mixed symmetry right below E_F becomes a $\bar{Y}_1$ SS, and crosses E_F to form an unoccupied $\bar{Y}_1$ SS with a rather large upward dispersion toward $\bar{M}$, as observed by experiment.[14] The other low-lying $\bar{Y}_2$ SS bands, extending about halfway from $\bar{M}$ and $\bar{X}$, consist of three SS not yet observed experimentally to the best of our knowledge. Several unoccupied SS and SR states mostly of $\bar{Y}_1$ symmetry are also seen near the absolute symmetry gaps in the conduction band. Previous calculation,[3] however, shows only one flat high-lying $\bar{Y}_1$ SS band at about $+1.2$ eV, in contrast to our results.

C. Layer density of states

Layer-projected densities of states (LDOS) provide useful information for single-particle spectra. In Fig. 5, we display the LDOS of the seven-layer Mo(001) slab. The two prominent peaks at -0.2 and -0.6 eV are associated with SS and SR states consisting of d orbitals which are well localized in the surface layer. It is interesting to note that the low-lying SR states of Mo(S) are accidentally located at the valleys, -2.4 and -3.3 eV, of Mo(C) to make the LDOS of Mo(S) nearly structureless. Furthermore, these SR states are hybridized with the states of Mo($S-1$), and cause the LDOS of Mo($S-1$) also to be structureless. One realizes that these SR states have small contributions from s or p orbitals, which are depicted as dashed curves. Most of the d orbitals closely follow the envelope of the total DOS for both occupied and unoccupied states.

IV. SUMMARY

We have calculated the electronic structure of an ideal Mo(001) surface, which reveals the detailed nature of the

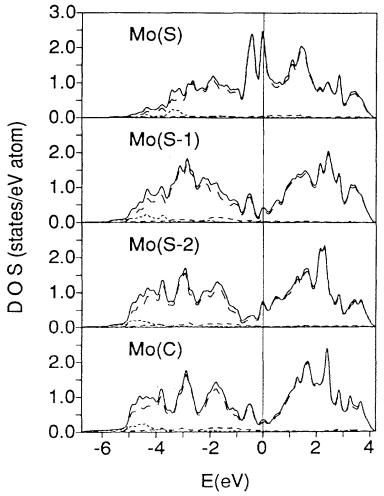

FIG. 5. Layer-projected density of states (LDOS) for a seven-layer Mo(001) film in states/eV atom. Note that the d orbitals closely follow the envelope of the total DOS for both occupied and unoccupied states. Contributions from s or p orbitals are depicted with dashed curves.

SS and SR states in the irreducible SBZ. We identify several true surface states such as the high-lying $\bar{\Sigma}_1$ SS, $\bar{\Delta}_1$ SS, $\bar{Y}_1$ SS just below E_F and the low-lying $\bar{Y}_2$ SS at about -2.5 eV at $\bar{M}$, and surface resonances such as high-lying $\bar{\Sigma}_2$ SR, $\bar{\Delta}_1$ SR, and the low-lying $\bar{\Sigma}_1$ SR, $\bar{\Delta}_1$ SR as discussed earlier. In particular, we also find SS's of mixed symmetry especially near the zone boundary $\bar{X}$.

Our results are in qualitative agreement with experimental measurements except several features such as Fermi wave-vector dimensions and band connectivity. The discrepancies are, in a sense, expected since such surface bands are closely related to the reconstruction of the surface. We should also point out that further ambiguity in accurate identification of the surface bands and symmetries comes from the fact that the experimental energy dispersions for the reconstructed Mo(001) surface are complicated by the two rotationally degenerated domains of the $c(2.2\times2.2)$ phase. In searching for theoretical evidence for a driving mechanism of the transition, it will be extremely useful to calculate the electronic susceptibility which might show a peak at the wave vector of the reconstruction, as for W(001).

ACKNOWLEDGMENTS

This work was supported in part by the Center for Advanced Materials Physics (CAMP), the Korean Ministry of Education through Basic Science Research Center at POSTECH, and by the University of Ulsan.

[1]Shang-Lin Weng, T. Gustafsson, and E. W. Plummer, Phys. Rev. Lett. **39**, 822 (1977).
[2]C. M. Bertoni, C. Calandra, and F. Manghi, Solid State Commun. **23**, 255 (1977).
[3]G. P. Kerker, K. M. Ho, and Marvin L. Cohen, Phys. Rev. Lett. **40**, 1593 (1978).
[4]H. Krakauer, M. Posternak, and A. J. Freeman, Phys. Rev. Lett. **43**, 1885 (1979).
[5]J. E. Inglesfield, J. Phys. C **12**, 149 (1979).
[6]J. C. Campuzao, J. E. Inglesfield, D. A. King, and C. Somerton, J. Phys. C **14**, 3099 (1981).
[7]E. Wimmer, H. Krakauer, M. Weinert, and A. J. Freeman, Phys. Rev. B **24**, 864 (1981).
[8]M. Posternak, H. Krakauer, A. J. Freeman, and D. D. Koelling, Phys. Rev. B **21**, 5601 (1980).
[9]P. C. Stephenson and D. W. Bullett, Surf. Sci. **139**, 1 (1984).
[10]L. F. Matteiss and D. R. Hamman, Phys. Rev. B **29**, 5372 (1984).
[11]T. E. Felter, R. A. Barker, and P. J. Estrup, Phys. Rev. Lett. **38**, 1138 (1977).
[12]M. K. Debe and D. A. King, Phys. Rev. Lett. **39**, 708 (1977).
[13]J. C. Campuzano, D. A. King, C. Somerton, and J. E. Inglesfield, Phys. Rev. Lett. **45**, 1649 (1980).
[14]Kevin E. Smith and Stephen D. Kevan, Phys. Rev. B **43**, 3986 (1991); **45**, 13 642 (1992), and references therein.
[15]Shang-Lin Weng, T. Gustafsson, and E. W. Plummer, Phys. Rev. Lett. **39**, 822 (1977); Phys. Rev. B **18**, 1718 (1978).
[16]J. W. Chung, K. S. Shin, D. H. Baek, C. Y. Kim, H. W. Kim, S. K. Lee, C. Y. Park, S. C. Hong, T. Kinoshida, A. Kakizaki, M. Watanabe, and T. Ishii, Phys. Rev. Lett. **69**, 2228 (1992).
[17]D. Singe and H. Krakauer, Phys. Rev. B **37**, 3999 (1988).
[18]K. S. Shin, C. Y. Kim, J. W. Chung, S. K. Lee, C. Y. Park, S. C. Hong, T. Kinoshida, A. Kakizaki, M. Watanabe, and T. Ishii (unpublished).
[19]M. L. Hildner, R. S. Daley, T. E. Felter, and P. J. Estrup, J. Vac. Sci. Technol. A **9**, 1604 (1991).
[20]C. Z. Wang, E. Tosatti, and A. Fasolino, Phys. Rev. Lett. **60**, 2661 (1988).
[21]X. W. Wang, C. T. Chan, K. M. Ho, and W. Weber, Phys. Rev. Lett. **60**, 2066 (1988).